



Nanocarnation-like Nickel Oxide Thin Film: Structural and Optical Properties

N. Parimon^{1,3,*}, M. H. Mamat^{1,2,*}, M. A. R. Abdullah¹, A. S. Ismail¹, W. R. W. Ahmad¹, I. B. Shameem Banu⁴, and M. Rusop^{1,2}

¹NANO-ElecTronic Centre (NET), Faculty of Electrical Engineering, Universiti Teknologi MARA (UiTM), 40450 Shah Alam, Selangor, Malaysia

²NANO-SciTech Centre (NST), Institute of Science (IOS), Universiti Teknologi MARA (UiTM), 40450 Shah Alam, Selangor, Malaysia

³ Faculty of Engineering, Universiti Malaysia Sabah, 88400 Kota Kinabalu, Sabah, Malaysia

⁴Department of Physics, B.S. Abdur Rahman Crescent Institute of Science & Technology, Vandalur, Chennai, 600 048, India

*Corresponding author E-mail: fara2012@ums.edu.my, mhmamat@salam.uitm.edu.my

Abstract

Herein, the structural and optical properties of highly porous nanocarnation-like nickel oxide (NiO) thin film in possibility of sensing applications were reported. The highly porous nanocarnation-like NiO was grown on indium tin oxide (ITO) glass substrates by using sonicated sol-gel immersion process. The grown film was characterized in details to examine the structural and optical properties using field emission scanning electron microscopy (FESEM), X-ray diffraction (XRD), Raman spectroscopy, and ultraviolet-visible-near infrared (UV-vis-NIR) spectroscopy, respectively. The XRD pattern reveals that the grown nanocarnation-like NiO film has crystalline NiO with a cubic structure. The UV-vis-NIR spectrum demonstrates that the average transmittance value of the sample in the visible region is approximately 48 % transmission. The results showed that, in view of highly porous nanocarnation-like NiO structure exhibited a great influence on its possibility for sensing applications.

Keywords: Nickel oxide (NiO); Thin Film; sol-gel; Structural Properties; Optical Properties

1. Introduction

Some metal oxides with semiconductor properties of n-type or p-type such as ZnO, TiO₂, Fe₂O₃, WO₃, CuO and NiO has been discussed extensively to be utilized as outstanding electron mediator for sensing membranes [1]. From previous researches, metal oxides have attained excellent consideration because of its terrific surface properties like high surface area, large pore volume, pore diameter, well-ordered pore channels and capillaries [2]. For example, the porous structures of metal oxides can be seen their utilization in wide sensing applications [3] including for gas [1, 4-7] and humidity [8, 9]. In addition, metal oxides have other important advantages such as low cost preparation, easy integration in electronic circuit, and controllable preparation process.

Meanwhile, the reports on p-type metal oxides semiconductors are relatively rare. Among all the p-type metal oxides, nickel oxide (NiO) which has a wide band gap (3.6 - 4.0 eV) is most preferable for widely used in various sensing applications because of the excellent chemical stability and high optical transparency [3]. In addition, NiO nanomaterial possess magnificent electrical conductivity, distinctly electro-active nature, low synthesis cost and a high surface to volume ratio [1]. Meanwhile, the sensing properties based on p-type oxide semiconductor materials are relatively poor compare to the n-type oxide semiconductor materials if both materials share similar morphologies and size [10]. This is based on the equation of $S_p = (S_n)^{1/2}$, where S_p and S_n are the chemical or gas sensitivities of the p-type and n-type oxide semiconductors, respectively. This equation evidently reveals that the fabrication of

p-type oxide semiconductor materials for high performance sensor applications remains a huge challenge. Therefore, the details study on fabrication processes and properties of nanostructured NiO provide interesting tasks toward improving the properties of p-type materials as a sensing membrane.

Although many techniques such as hydrothermal [1, 5, 6], chemical spray pyrolysis (CSP) and chemical bath deposition (CBD) [7], electrospinning [8, 9], and sol-gel [11] have been put widely into the synthesis of NiO nanostructures, it remains rare for researchers using a facile route of sonicated sol-gel immersion method. In addition to simple techniques, it is important because the design and preparation of nanostructured metal oxides with various morphologies can effectively improve the sensing properties due to their high surface area [12]. Accordingly, this NiO thin film was prepared on indium tin oxide (ITO) glass substrates in the present study for possibility in sensing applications.

2. Experimental Details

For this work, nanocarnation-like NiO thin film was successfully prepared on ITO glass substrates. The fabrication involved sonicated sol-gel immersion method using a precursor solution of nickel nitrate hexahydrate. Prior to the growth process, ITO glass was cleaned using solutions of ethanol, acetone, and de-ionized (DI) water in the ultrasonic bath (Hwasin Technology PowerSonic 405, 40k Hz) for 15 minutes each. Furthermore, the ITO glass is blown using nitrogen gas for drying. To grow nanocarnation-like NiO thin film, a solution consisting of 0.2M nickel (II) nitrate



hexahydrate ($\text{Ni}(\text{NO}_3)_2 \cdot 6\text{H}_2\text{O}$) and 0.2M hexamethylenetetramine (HMT) ($\text{C}_6\text{H}_{12}\text{N}_4$) were prepared in a beaker filled with 200 ml DI water. The solution then went through sonication process using ultrasonic bath for 30 minutes. Next, the solution was stirred for 45 minutes at constant speed of 300 rpm in ambient. Then, the solution was transferred to the Schott bottle, where the ITO glass substrate was positioned at the bottom. Afterward, the bottle was immersed in water bath instrument for 2 hours at temperature of 95 °C. After the immersion process, the ITO glass deposited with NiO thin film was taken out from the bottle and rinsed with DI water. The sample was further blown with nitrogen gas for drying process. Then, the sample was pre-baked in a furnace for 15 minutes at 150 °C followed by annealing process at temperature of 500 °C for 1 hour.

The sample was characterized using field emission scanning electron microscopy (FESEM, JEOL JSM-7600F) for the surface morphological studies. The crystallinity of the sample was investigated using X-ray diffraction (PANalytical X'Pert PRO). The structural analysis of the sample was also conducted by using Raman spectroscopy (Horiba Jobin Yvon-79 DU420A-OE-325). The Raman measurement was conducted using an excitation source of 514 nm Ar^+ ion laser. The optical properties of the grown sample were characterized using ultraviolet–visible–near infrared (UV–vis–NIR) spectrophotometer (Varian Cary 5000). Summarization of the experiment processes in a flow chart is shown in Fig. 1.

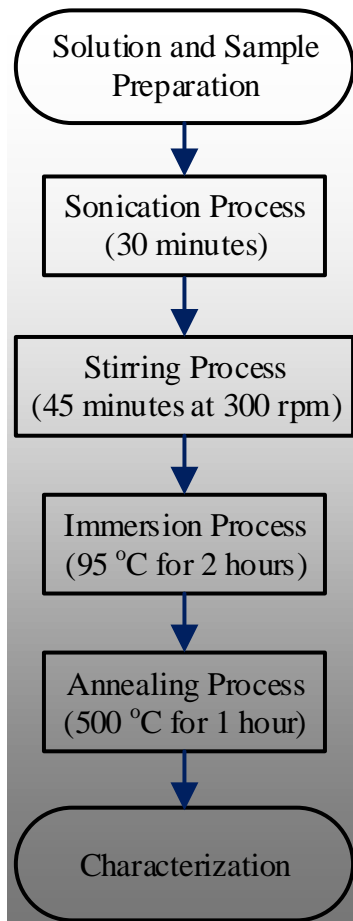


Fig. 1: A general procedure showing various steps for the synthesizing of nanocarnation-like NiO thin film.

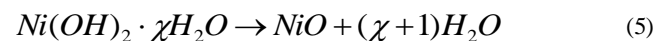
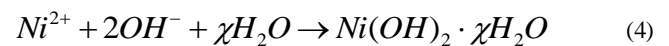
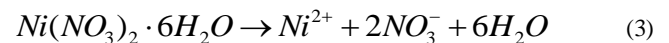
3. Results and Analysis

3.1. FESEM observation

The surface morphology images and micro structural features of NiO film on ITO-coated glass substrates were investigated in detail by FESEM. As depicted in Fig. 2, (a), (b), (c), and (d) the panoramic FESEM images are arranged according to the magnifi-

cation of 10,000×, 30,000×, 50,000× and 100,000×, respectively. As observed from the FESEM images in Fig. 2(a), the films exhibit unique structures called nanocarnation-like NiO with high porous channel densities. These films reveal porous structure of well-connected particles to form nanocarnation-like structure. We can see that the microstructure of pure NiO is highly porous nanosheets. The diameter of individual nanocarnation-like NiO is approximately 1.5 μm. The FESEM images in Fig. 2(b) and 2(c) revealed that the nanocarnation-like NiO was constructed from NiO nanolayers. The nanocarnation-like NiO was assembled by a plenty of two-dimensional curving NiO nanolayers forming a highly porous microsphere. Meanwhile, the two-dimensional nanolayer was fabricated from NiO nanocrystallite chains, which form unique and porous network layers as can be observed in Fig. 2(d).

The chemical reactions for the formation of nanocarnation-like NiO using sonicated sol-gel immersion method can be described by the following equations [1]:



Preliminary, the HMT decomposes into formaldehyde (HCHO) and ammonia (NH_3) in the water medium as described in Eq. 1. These chemical substances provide an alkaline environment to the solution, which enhance the growth of nanostructures. Besides, these reagents also act as the surfactant agent to the Ni^{2+} ions for polymerization process.

According to Jiang et al., NH_3 forms a complex molecules with Ni^{2+} ions, which subsequently reduces the concentration of Ni^{2+} ions in the solution [13]. Therefore, the growth rate of the crystal is reduced, which enables the formation of thin two-dimensional nanolayers. The HMT undergoes a hydrolysis process as the reaction proceeds, which produces more OH^- ions in the solution. This condition is favorable for the formation of two-dimensional $\text{Ni}(\text{OH})_2$ on the ITO glass. This hydrolysis process of the HMT can be described in Eq. 2, where the by-product of Eq. 1 in form of NH_3 reacts with water to produce NH_4^+ and OH^- ions in the process. Therefore, HMT acts as a pH buffer in the solution by providing NH_3 at a slow rate and in controlled supply. Simultaneously, the $\text{Ni}(\text{NO}_3)_2 \cdot 6\text{H}_2\text{O}$ decomposes into Ni^{2+} ion, NO_3^- ion, and water in the solution as presented in Eq. 3. Successively, the Ni^{2+} ion reacts with NO_3^- ion and water molecules in the presence of thermal energy to form $\text{Ni}(\text{OH})_2 \cdot \chi\text{H}_2\text{O}$ in the process, which then condenses on the ITO glass.

The reaction is shown in Eq. 4. The remaining HMT, which are not involved in the NH_3 decomposition, may adsorbed on (001) plane of $\text{Ni}(\text{OH})_2 \cdot \chi\text{H}_2\text{O}$. This condition inhibited the growth of $\text{Ni}(\text{OH})_2 \cdot \chi\text{H}_2\text{O}$ at (001) plane to form thin two-dimensional nanolayers. To minimize the overall surface energy, the thin two-dimensional $\text{Ni}(\text{OH})_2 \cdot \chi\text{H}_2\text{O}$ nanolayers would self-aggregate to form nanocarnation-like structure. Subsequently, some of the $\text{Ni}(\text{OH})_2 \cdot \chi\text{H}_2\text{O}$ structures on ITO glass decomposes into NiO nanostructure as described in Eq. 5 due to the supplied thermal energy during immersion process. Upon annealing process at 500°C, a complete conversion of $\text{Ni}(\text{OH})_2 \cdot \chi\text{H}_2\text{O}$ into NiO is occurred as a result of sufficient thermal energy supplied to the system. This conversion into NiO crystal was confirmed by the XRD data.

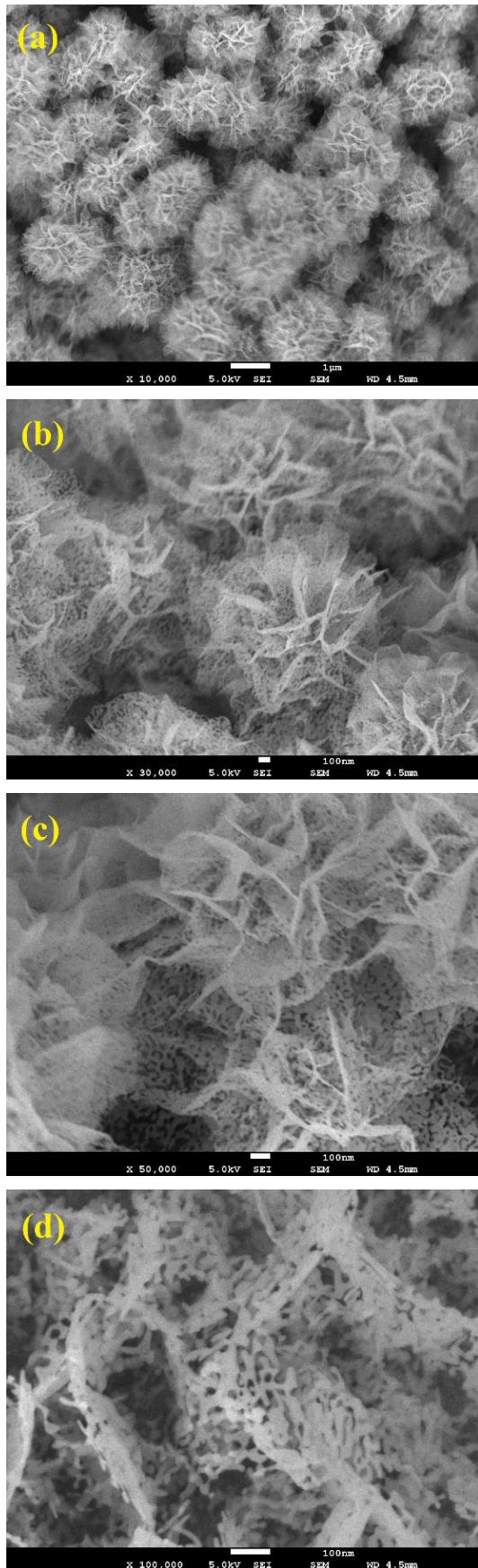


Fig. 2: The FESEM images of nanocarnation-like NiO thin film with different magnification of (a) 10,000 \times (b) 30,000 \times (c) 50,000 \times , and (d) 100,000 \times .

3.2. XRD analysis

The XRD pattern for nanocarnation-like NiO film grown on ITO glass substrates is shown in Fig. 3. The XRD pattern indicates that

NiO film displays polycrystalline structure, which can be indexed to the cubic type of β -NiO (JCPDS NO.47-1049). The diffraction patterns revealed that NiO film shows peaks at 2θ values of approximately 37.7 $^\circ$, 43.7 $^\circ$, 63.4 $^\circ$, 75.8 $^\circ$ and 79.7 $^\circ$ which were indexed to (111), (200), (220), (311), and (222) crystal planes, respectively. Meanwhile, the diffraction peaks labelled with diamond belong to SnO_2 peaks from the ITO. The XRD examination confirmed that the results indicate the crystalline of NiO structure during immersion at 95 $^\circ\text{C}$ and calcination at 500 $^\circ\text{C}$. The XRD pattern also reveals that no other diffraction peaks associated with $\text{Ni}(\text{OH})_2$ or other phases were observed in the pattern. This result further confirmed that the grown NiO film consists of pure NiO structure and prove that the $\text{Ni}(\text{OH})_2 \cdot \gamma\text{H}_2\text{O}$ was completely converted into NiO. The impurity from other substance except the contribution from the ITO substrate is not significant and could not be detected in the pattern up to the detection limit of the X-ray diffraction equipment. According to Dam et al., the hydroxide groups were completely detached from NiO film when the heat treatment was applied at temperature of 270 $^\circ\text{C}$ [14].

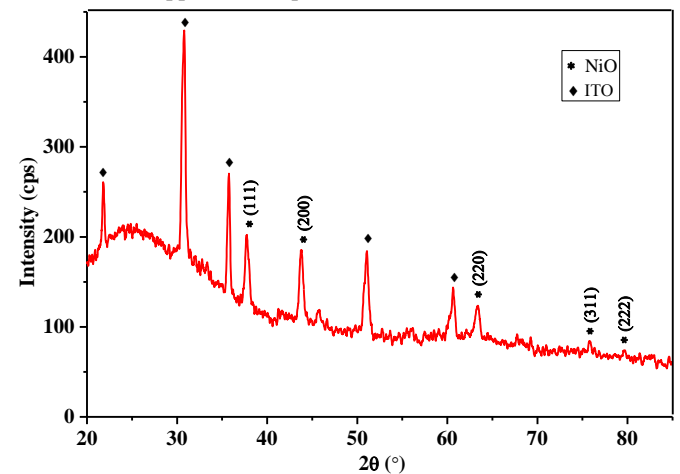


Fig. 3: The XRD pattern of nanocarnation-like NiO film.

3.3. Raman spectroscopy

The Raman measurement was conducted in order to further investigate the structural properties of nanocarnation-like NiO film. The Raman spectrum of nanocarnation-like NiO film is shown in Fig. 4. The spectrum was dominated by numerous of NiO characteristic peaks. The first vibrational band of NiO, assigned to one-phonon (1P) transverse optical (TO) and 1P longitudinal optical (LO) modes were observed at Raman shift of approximately 463 cm^{-1} and 492 cm^{-1} [15]. The vibrational peak at 554 cm^{-1} is assigned to the Ni-O stretching mode, which involves Ni^{2+} and O^{2-} species that are not linked to a proton [16]. The presence of these first order Raman scattering peaks indicate that structural imperfection of NiO occurs, which contributed from the structural disorder by nickel interstitial, oxygen vacancies, and surface effects [17-19]. Also, there is a strong 2LO phonon mode located at 1093 cm^{-1} due to the vibration of Ni-O bond. In between, there is two-phonon (2P) two transverse optical (2TO) stretching mode at 810 cm^{-1} with low intensities. In the present study, two magnons (2M) excitation peak, which normally located at 1550 cm^{-1} [20, 21], was not observed in the Raman spectrum to indicate that the prepared nanocarnation-like NiO film does not has antiferromagnetic properties at room temperature. This result also indicate that the nanocarnation-like NiO film exhibits super-paramagnetic properties due to the small crystallite size and high density of structural disorder [18].

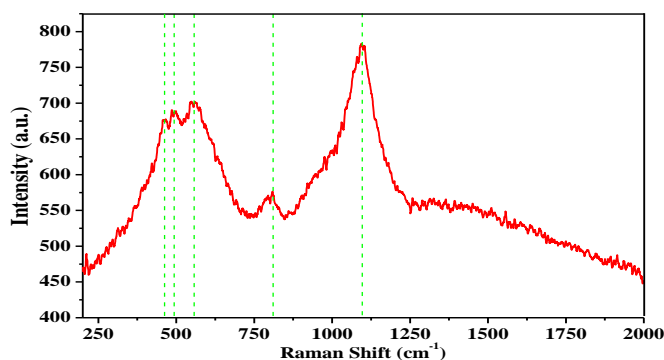


Fig. 4: Raman spectrum of nanocarnation-like NiO film

3.4. UV-vis-NIR spectroscopy

Fig. 5 demonstrates optical transmittance of the nanocarnation-like NiO thin film prepared using sonicated sol-gel immersion method. The optical transmittance measurement was carried out in the ranges of wavelength from 300 nm to 1000 nm. From the transmittance plot, we can clearly observe that the nanocarnation-like NiO exhibit moderate transparency. The transmittance extends to 50 % or less in the ultraviolet (UV) and visible regions. The average transmittance value of the film in the visible region (400 - 800 nm) was estimated to be 48 %. This lower transmittance percentage may be depending on the thickness of nanocarnation-like NiO film. In addition, the optical scattering occurrence in the nanocarnation-like NiO film may be one of the factors to this transmittance result.

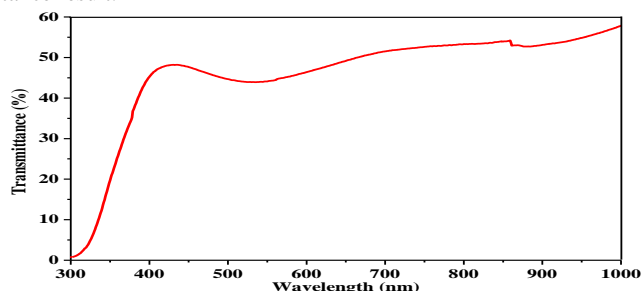


Fig. 5: The transmittance properties of NiO in the UV visible regions

4. Conclusion

The synthesis of porous morphology nanocarnation-like NiO has been successfully conducted via sonicated sol-gel immersion method. The highly porous nanocarnation-like NiO was characterized by various techniques which confirmed the formation of well-crystalline cubic phase, pure, and high density growth of nanocarnation-like NiO. The XRD pattern reveals that the grown NiO sample has NiO polycrystalline structure. The Raman analysis shows that nanocarnation-like NiO film has pure NiO characteristic peaks, which support the XRD data. The transmittance plot shows that the transparency of highly porous nanocarnation-like NiO is approximately 48 % in the visible region. In summary, the exposure of high surface area nanocarnation-like NiO thin film with high porosity represent a valuable way for producing high performance and sensitivity sensing applications in the future.

Acknowledgement

This work is financially supported by REI grant (600-IRMI/REI 5/3 (017/2018)). The work is also supported by ASEAN-India Research & Training Fellowship (IMRC/AISTDF/R&D/P-1/2017). The authors would like to thank Ministry of Higher Education, Malaysia, Faculty of Electrical Engineering and Research Management and Innovation (IRMI) of UiTM for their support of this research.

References

- [1] Z. Qu, U. Ahmad, S. E. Mehdi, A. Aziz, X. Lingna, G. Yingang, A. I. Ahmed, K. Rajesh & S. Baskoutas (2018), Fabrication and characterization of highly sensitive and selective sensors based on porous NiO nanodisks. *Sensors and Actuators B: Chemical* 259, 604-615.
- [2] D. Ahirwar, M. Bano, I. Khan, M. U.-D. Sheikh, M. Thomas & F. Khan (2018), Fabrication of hierarchically mesoporous NiO nanostructures and their role in heterogeneous photocatalysis and sensing activity. *Journal of Materials Science: Materials in Electronics* 29, 5768-5781.
- [3] S. Akinkuade, B. Mwankemwa, J. Nel & W. Meyer (2018), Structural, optical and electrical characteristics of nickel oxide thin films synthesised through chemical processing method. *Physica B: Condensed Matter* 535, 24-28.
- [4] S. Leonardi (2017), Two-Dimensional Zinc Oxide Nanostructures for Gas Sensor Applications. *Chemosensors* 5, 17, 28.
- [5] Y. Lu, Y. Ma, S. Ma & S. Yan (2017), Hierarchical Heterostructure of Porous NiO Nanosheets on Flower-like ZnO Assembled by Hexagonal Nanorods for High-performance Gas Sensor. *Ceramics International* 43, 7508-7515.
- [6] R. Miao, W. Zeng & Q. Gao (2017), Hydrothermal synthesis of novel NiO nanoflowers assisted with CTAB and SDS respectively and their gas-sensing properties. *Materials Letters* 186, 175-177.
- [7] M. M. Gomaa, G. RezaYazdi, M. Rodner, G. Greczynski, M. Boshita, M. B. S. Osman, V. Khranovskyy, J. Eriksson & R. Yakimova (2018), Exploring NiO nanosize structures for ammonia sensing. *Journal of Materials Science: Materials in Electronics* 29, 11870-11877.
- [8] D. Li, Y. Li, F. Li, J. Zhang, X. Zhu, S. Wen & S. Ruan (2015), Humidity sensing properties of MoO₃-NiO nanocomposite materials. *Ceramics International* 41, 4348-4353.
- [9] P. Pascariu, A. Airinei, N. Olaru, I. Petrilă, V. Nica, L. Sacarescu, F. Tudorache (2016), Microstructure, electrical and humidity sensor properties of electrospun NiO-SnO₂ nanofibers. *Sensors and Actuators B: Chemical* 222, 1024-1031.
- [10] M. Hübner, C. E. Simion, A. Tomescu-Stănoiu, S. Pokhrel, N. Bârsan & U. Weimar (2011), Influence of humidity on CO sensing with p-type CuO thick film gas sensors. *Sensors and Actuators B: Chemical* 153, 347-353.
- [11] L. G. Teoh & K.-D. Li (2012), Synthesis and Characterization of NiO Nanoparticles by Sol-Gel Method. *Materials Transactions* 53, 2135-2140.
- [12] H. Gao, D. Wei, P. Lin, C. Liu, P. Sun, K. Shimanoe, N. Yamazoe & G. Lu (2017), The design of excellent xylene gas sensor using Sn-doped NiO hierarchical nanostructure. *Sensors and Actuators B: Chemical* 253, 1152-1162.
- [13] H. Jiang, T. Zhao, C. Li & J. Ma (2011), Hierarchical self-assembly of ultrathin nickel hydroxide nanoflakes for high-performance supercapacitors. *Journal of Materials Chemistry* 21, 11, 3818-3823.
- [14] D. T. Dam, X. Wang & J.-M. Lee (2013), Mesoporous ITO/NiO with a core/shell structure for supercapacitors. *Nano Energy*, 2, 6, 1303-1313.
- [15] P. Bose, S. Ghosh, S. Basak & M. K. Naskar (2016), A facile synthesis of mesoporous NiO nanosheets and their application in CO oxidation. *Journal of Asian Ceramic Societies*, 4, 1, 1-5.
- [16] S. Deabate, F. Fourgeot & F. Henn (2000), X-ray diffraction and micro-Raman spectroscopy analysis of new nickel hydroxide obtained by electroanalysis. *Journal of Power Sources*, 87, 1, 125-136.
- [17] N. P. Kiran, M. P. Deshpande, C. Krishna, R. Piyush, S. Vasant, P. Swati & S. H. Chaki (2017), Synthesis, structural and photoluminescence properties of nano-crystalline Cu doped NiO. *Materials Research Express* 4, 10, 105027.
- [18] P. Ravikumar, B. Kisan & A. Perumal (2015), Enhanced room temperature ferromagnetism in antiferromagnetic NiO nanoparticles. *AIP Advances*, 5, 8, 087116.
- [19] S. Liu, J. Jia, J. Wang, S. Liu, X. Wang, H. Song and X. Hu (2012), Synthesis of Fe-doped NiO nanofibers using electrospinning method and their ferromagnetic properties. *Journal of Magnetism and Magnetic Materials* 324, 13, 2070-2074.
- [20] F. T. Thema, E. Manikandan, A. Gurib-Fakim & M. Maaza (2016), Single phase Bunsenite NiO nanoparticles green synthesis by Agathosma betulina natural extract. *Journal of Alloys and Compounds* 657, 655-661.
- [21] M. Ben Amor, A. Boukchachem, A. Labidi, K. Boubaker, and M. Amlouk (2017), Physical investigations on Cd doped NiO thin films along with ethanol sensing at relatively low temperature. *Journal of Alloys and Compounds* 693, 490-499.